Revelation and Science
Vol. 15, No. 02 (1446H/2025) 21-30

MHD MIXED CONVECTIVE FLOW OF VISCOUS FLUID IN SINUSOIDAL CHANNEL

Ahmad Danish Afiq Suhardi[1], Nor Raihan Mohamad Asimoni[1*], Sharidan Shafie[2]
[1] Kulliyyah of Science, International Islamic University Malaysia (IIUM)
[2] Faculty of Science, Universiti Teknologi Malaysia (UTM).

Abstract
This research paper aims to investigate the influence of magnetohydrodynamics (MHD), Richardson's number, wave amplitude, and the undulation number of a wavy surface on the velocity and temperature profiles of a viscous fluid within a wavy channel. The weak formulation is applied to the continuity equation, momentum equation, and energy equation. Then, the problem is solved numerically with the help of the automated solution technique FEniCS and plotted using matplotlib. This study revealed that the velocity profiles increase with the increment of Richardson number, wave amplitude, and undulation number of wavy surfaces. However, the velocity profiles decrease as the magnetic parameters increase. The result showed that magnetic parameters and Richardson number give no significant impact to the temperature profile with the exception of wave amplitude and the undulation number, where the temperature profile increases.
Keywords: MHD, mixed convective flow, sinusoidal channel, FEniCS

Introduction

Research on the velocity and temperature profiles of fluid in a corrugated channel has been well-established. Izumi *et al*. (1983) and Their *et al*. (2023) agreed that corrugated channels enhanced the heat transfer rate. Zhang *et al*. (2004) mentioned in their literature that wall corrugations created a consistent swirl or vortex in the trough areas of the corrugated wall. Comparable effects were reported by Ahmed *et al*. (2015), as they identified a recirculation zone that appeared within the corrugated channel but none in a straight channel. As a result, these authors concluded that adding corrugated walls enhanced the fluid mixing between hot fluid and cold fluid near the channel walls.

Abu Talib and Hilo (2021) investigated the effect of the amplitude of trapezoidal-corrugated walls on the fluid flow and the heat transfer. They discovered that amplifying the amplitude led to significant increase in the velocity streamline. Similarly, Lahlou *et al*. (2024) revealed that increasing the sinusoidal-corrugated wall amplitude impacted the flow pattern. Abu Talib and Hilo (2021) mentioned that the heat transfer was affected by the corrugated walls' amplitude. This phenomenon was supported by Mehta *et al*. (2022), who suggested that the higher the amplitude, the greater the temperature gradients, which then improved the heat transfer. However, Lahlou *et al*. (2024) suggested

[*] *Corresponding Author:*
Nor Raihan Mohamad Asimoni
Kulliyyah of Science, International Islamic University Malaysia (IIUM)
Email: raihanasimoni@iium.edu.my

that heat transfer improved due to the increment of fluid-wall thermal contact.

Hussain *et al*. (2023) studied the influence of the Richardson number on the flow patterns and the temperature distributions of Ag-MgO-water hybrid nanofluid in a channel with a circular cylinder as well as a cavity that contained the wavy porous layer on the lower wall. They revealed that a small convection cell appeared when the forced convection ($Ri < 1$) was governed. The authors further noted that, as the Richardson number increases, the convective cell expands due to greater buoyancy force, and the thermal behavior near the lower cavity is enhanced as the temperature features group together near the lower boundaries.

Sinusoidal-corrugated channels, known as wavy channels, are one of the popular geometries for corrugated channels. Pati *et al*. (2017) stated that wavy channels can be categorized into two types, which are raccoon channel (symmetric channel) and serpentine channel (asymmetric channel). However, serpentine channels exhibit significantly higher efficiency compared to symmetrical channels. Jalili *et al*. (2024) investigated the effects of MHD on the fluid flow in an asymmetrical wavy channel made of porous media. They remarked that as the Hartmann number increased, the real values of fluid velocity decreased.

Alsabery *et al*. (2022) scrutinized the forced convection of turbulent flow in a wavy channel. They analysed the influence of the waviness number and wavy wall amplitude on the velocity and heat transfer. They ascertained that the formation of recirculation within the wave troughs appeared as the waviness number increased. Additionally, they stated that the presence of rippling allows the fluid flow to escalate. A comparable study by Madlool *et al*. (2023) also detected a similar result. They discovered that as the undulation numbers rose, the maximum magnitude of velocity was observed at the center of the channel.

FEniCS is an open-source software program that solves PDEs using the finite element method. Logg *et al*. (2012) stated that FEniCS can be programmed with C++ and Python. They mentioned that FEniCS in Python programming is simple and straightforward for beginners while maintaining optimal performance. Research conducted by Asimoni *et al*. (2018) used FEniCS to study the MHD forced convective flow past a vertical plate. The authors asserted that the domain is automatically discretized, and the problem can be solved directly in vector form. These are the advantages of using FEniCS.

Motivated by the previous studies, this research will focus on the fluid flow of a viscous fluid in a sinusoidal-corrugated channel with the presence of a magnetic field. This research will be solved numerically using the finite element method with the help of the automated solution technique FEniCS.

Mathematical Formulation

As shown in Figure 1, the viscous fluid flows in a wavy channel where the lower wavy surface is hot, and the upper wavy surface has no change in temperature. The fluid enters from the left side of the channel with the initial velocity of $\mathbf{u}_{in} = (0.5, 0)$ and with the presence of magnetic field, β_0.

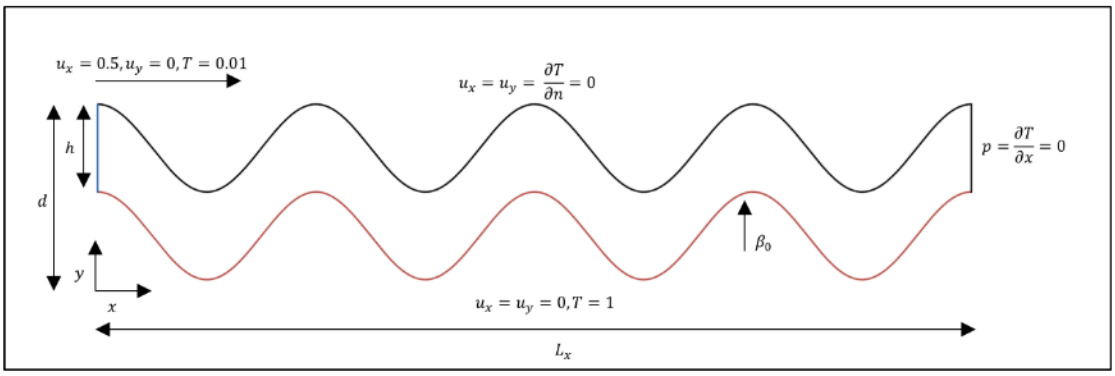

Figure 1: Configuration with boundary conditions

The non-dimensionalized form of governing equations are based on the modification of Iwatsu *et al.* (1993) Boussinesq approximation of incompressible Navier-Stokes equations with incorporate MHD and Richardson number:

The continuity equation:

$$\nabla \cdot \mathbf{u} = 0, \tag{1}$$

The time independent momentum equation:

$$(\mathbf{u} \cdot \nabla)\mathbf{u} = -\nabla p + \frac{1}{\mathrm{Re}} \Delta \mathbf{u} + Ri \cdot T\mathbf{e} - M\mathbf{u}\,, \tag{2}$$

The time independent energy equation:

$$\mathbf{u} \cdot \nabla T = \frac{1}{\mathrm{Pr} \cdot \mathrm{Re}} \Delta T\,, \tag{3}$$

With the corresponding non-dimensionalized parameters:

$$\mathrm{Re} = \frac{uL}{\nu}, \mathrm{Pr} = \frac{\nu}{\alpha}, Ri = \frac{\mathrm{g}\beta_0(\mathrm{T}_{hot} - T_{ref})L}{u^2}, \tag{4}$$

where $\mathbf{u} = (u_x, u_y)$ is the fluid velocity, T is the temperature, p is the pressure, Re is Reynolds number, Ri is Richardson number, Pr is Prandtl number, M is the magnetic parameter and $\mathbf{e} = (0,1)$ is a unit vector in the direction of the buoyancy force, u is the characteristic velocity, L is the characteristic length of the channel, ν is the kinematic viscosity, α is the thermal diffusivity, g is the acceleration due to gravity, β_0 is the magnetic field strength, T_{hot} is the wavy-wall hot temperature, and T_{ref} is the reference temperature.

The boundary conditions are the modifications from Madlool *et al.* (2023):

At the hot lower wavy surface:

$$\mathbf{u} = (0,0), \quad T = 1, \quad 0 < x < 2, \quad y = h - A(1 - \cos(N\pi x))\,,$$

At the cold inlet left surface:

$$\mathbf{u} = (0.5, 0), \quad T = 0.01, \quad x = 0, \quad d - h < y < d,$$

At the adiabatic upper wavy surface:

$$\mathbf{u} = (0, 0), \quad \frac{\partial T}{\partial n} = 0, \quad 0 < x < 2, \quad y = d - A(1 - \cos(N\pi x)),$$

At the adiabatic outlet right surface:

$$p = 0, \quad \frac{\partial T}{\partial x} = 0, \quad x = 2, \quad d - h < y < d. \tag{5}$$

where A is the wavy wall amplitude, and N is the undulation number of wavy surfaces, and $\frac{\partial}{\partial n}$ is the normal derivative with n is the exterior unit normal to the surfaces.

The weak formulation or the variational formulation must be applied to the partial differential equations (PDEs) in order to employ the finite element method. The standard Galerkin's method, as described by Larson and Bengzon (2013), involves multiplying the PDEs by their corresponding test functions and integrating them over the domain. Applying the standard Galerkin's method to the Eq. (1), Eq. (2), and Eq. (3) with the corresponding test functions q, $\mathbf{v}$, and s to obtained the weak formulation as presented in Eq. (6), Eq. (7) and Eq. (8):

$$\int_{\Omega} (\nabla \cdot \mathbf{u})\, q \, dx = 0, \tag{6}$$

$$\int_{\Omega} (\mathbf{u} \cdot \nabla)\mathbf{u} \cdot \mathbf{v} \, dx - \int_{\Omega} p\,(\nabla \cdot \mathbf{v}) \, dx + \int_{\Omega} \frac{1}{\mathrm{Re}} (\nabla \mathbf{u} \cdot \nabla \mathbf{v}) \, dx - \int_{\Omega} Ri \cdot T(\mathbf{e} \cdot \mathbf{v}) \, dx + \int_{\Omega} M(\mathbf{u} \cdot \mathbf{v}) \, dx = 0, \tag{7}$$

$$\int_{\Omega} (\mathbf{u} \cdot \nabla T)\, s \, dx + \int_{\Omega} \frac{1}{\mathrm{Pr} \cdot \mathrm{Re}} (\nabla T \cdot \nabla s) \, dx = 0. \tag{8}$$

Eq. (6), Eq. (7), and Eq. (8) will be coupled together and will be solved using the Newton-Raphson method with the help of automated solution technique FEniCS. The results will plot with Matplotlib

.

Results and Discussion

The computational validation will be verified with the result from Madlool *et al*. (2023). Eq. (2) will be reduced with the absence of magnetic parameters, M. Since the authors studied on the force convective flow, therefore the Richardson number is chosen such that $Ri < 1$. However, the equations used by authors never had the term with Richardson number; therefore, we will omit the term with Richardson number. The Prandtl number however is specified as $\mathrm{Pr} = 4.623$. The computations conducted with the set of values for Reynolds number, $\mathrm{Re} = \{10, 50, 100\}$. The comparisons are solely based on the plotting of the velocity in which the

higher velocity region is observed at the center of the channel and the contour of the temperature as shown in Figure 2 and Figure 3, respectively.

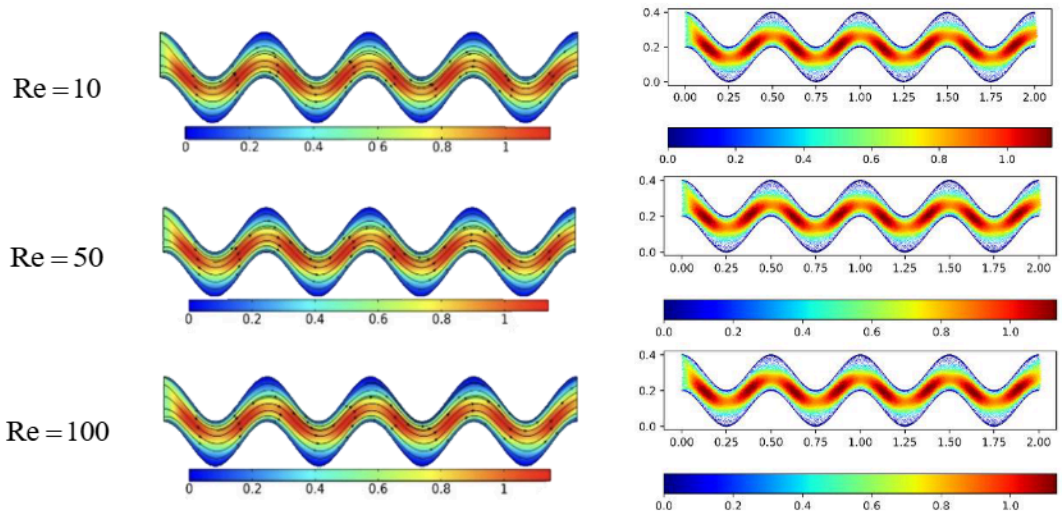

Figure 2: Comparison of velocity profiles between (a) Madlool *et al*. (2023) paper with (b) present

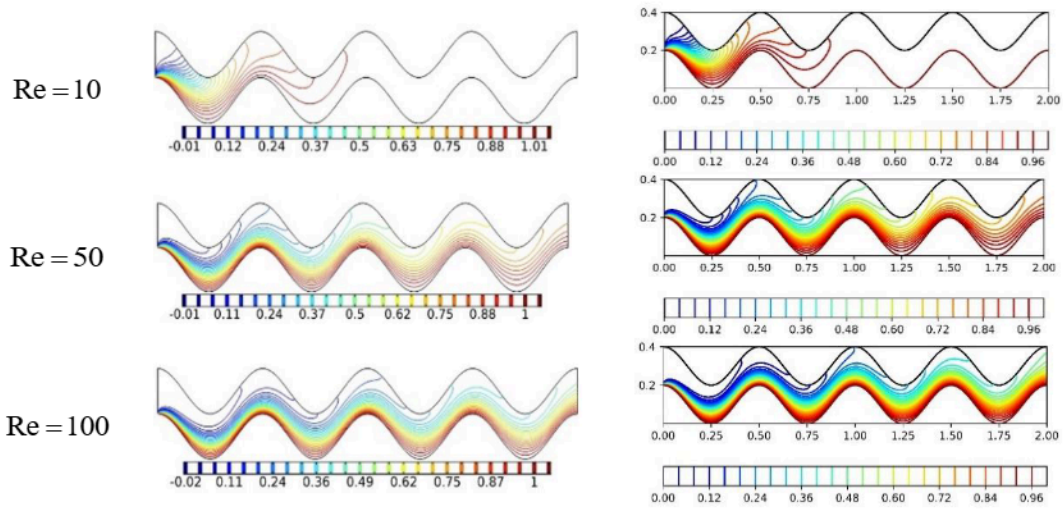

Figure 3: Comparison contour plot for temperature between (a) Madlool *et al*. (2023) paper with (b) present

The results for the velocity and the temperature profiles from the FEniCS simulation are presented. The velocity and temperature profiles are given for different in magnetic parameters ($M = 25, 50, 75, 100$), Richardson number ($Ri = 0.01, 1, 10$), wavy wall amplitudes ($A = 0.01, 0.05, 0.15, 0.185$), and undulation numbers of wavy surfaces ($N = 2, 4, 6, 8$) at fixed parameters $\mathrm{Pr} = 7$ and $\mathrm{Re} = 100$. Figure 4 displays the velocity and the temperature profiles for

different magnetic parameters with constant $Ri = 1$, $N = 4$, and $A = 0.1$. At low magnetic field, $M = 25$, from Figure 4(a), the fluid had a high velocity at the channel's centerline. Moreover, it could be seen in Figure 4(a) that the velocity of the fluid at the centerline decreased as the magnetic parameters increased based on the color concentration of the vector and the maximum value of the color bar. It was implied that the maximum value of velocity decreased. Consequently, increasing the magnetic parameter reduced the velocity profiles. Figure 4(b) revealed that the temperature profile followed the same behavior and pattern as the magnetic parameter increased. As a result, the temperature profile showed no significant impact as the magnetic parameter increased.

The velocity and the temperature profiles with different types of convection that are forced convective flow ($Ri < 1$), natural convective flow ($Ri > 1$), and mixed convective flow ($Ri = 1$) with constant $N = 4$, $A = 0.1$, and $M = 70$, are depicted in Figure 5. As shown in Figure 5(a), the velocity profiles of the fluid flow with $Ri = 0.01$ and the fluid flow with $Ri = 1$ exhibited unnoticeable changes in the behavior of the fluid flow. However, there were noticeable changes in the velocity of the fluid with $Ri = 10$. It could be perceived that the velocity of the fluid with $Ri = 10$ declined when sliding down and ascending through the channel walls by observing the color concentration of the vector. Nonetheless, the range of the color bar for the fluid with $Ri = 10$ grew slightly compared to fluid with $Ri = 0.01$ and $Ri = 1$. This indicated that the maximum velocity of the fluid flow increased slightly. Hence, the velocity profiles increased as there was a rise in the Richardson number. In Figure 5(b),the temperature profiles manifested the same behavior and pattern that is the fluid starting to heat up as it came closer to the outlet. Therefore, there was no significant impact on the temperature profiles as the Richardson number rose.

Figure 6 shows the velocity and temperature profiles with varying wave amplitudes and constant $Ri = 1$, $N = 4$, and $M = 80$. Referring to Figure 6(a), it could be seen that at the wavy wall crests, the vortex zone emerged as the wavy wall amplitude amplified. Furthermore, the color bar revealed a significant rise in the velocity as the wavy wall amplitude increased. Thus, increasing the wavy wall amplitude enhanced the velocity profiles. In Figure 6(b), it was evident that the temperature profiles elevated as the wavy wall amplitudes increased. At wave amplitude $A = 0.185$, an increment in the hot fluid movement to the upper wavy wall was observed as the temperature began to rise more quickly starting from $x = 1.00$. This phenomenon occurred because higher friction developed between the fluid and the wavy channel walls, thus enhancing the movement of the hot fluid. Hence, the greater the wave amplitude, the greater the temperature profiles.

Figure 7 demonstrates the velocity and the temperature profiles for different undulation numbers of wavy surfaces with $Ri = 1$, $A = 0.1$, and $M = 80$. From Figure 7(a), it was discovered that the recirculation zone appeared at the wavy wall crests, and the thickness of the zone grew as the undulation number increased, judging from the maximum magnitude of the color bar. Additionally, it could be observed that increasing the undulation number, the fluid pattern curled. It is aligned with the study by Madlool *et al*.

(2023) which stated that the flows become distorted, and it get stronger as N increased. As a result, there was a rise in the velocity profiles as the undulation number elevated. On the other hand, Figure 7(b) exhibited the same characteristics and behavior of the temperature profile in which the fluid started to get warmer at the right side of the channel. At $N=6$, the temperature of the fluid began to increase at around $x=1.5$ in comparison with the flow with $N=8$, where the fluid started to become warmer around $x=1.25$. This happened due to the growth in the interaction between the fluid and the wavy walls, thus improving the friction between the walls and the fluid. Therefore, a rise in the undulation number of the wavy surfaces enhanced the temperature profile of the fluid.

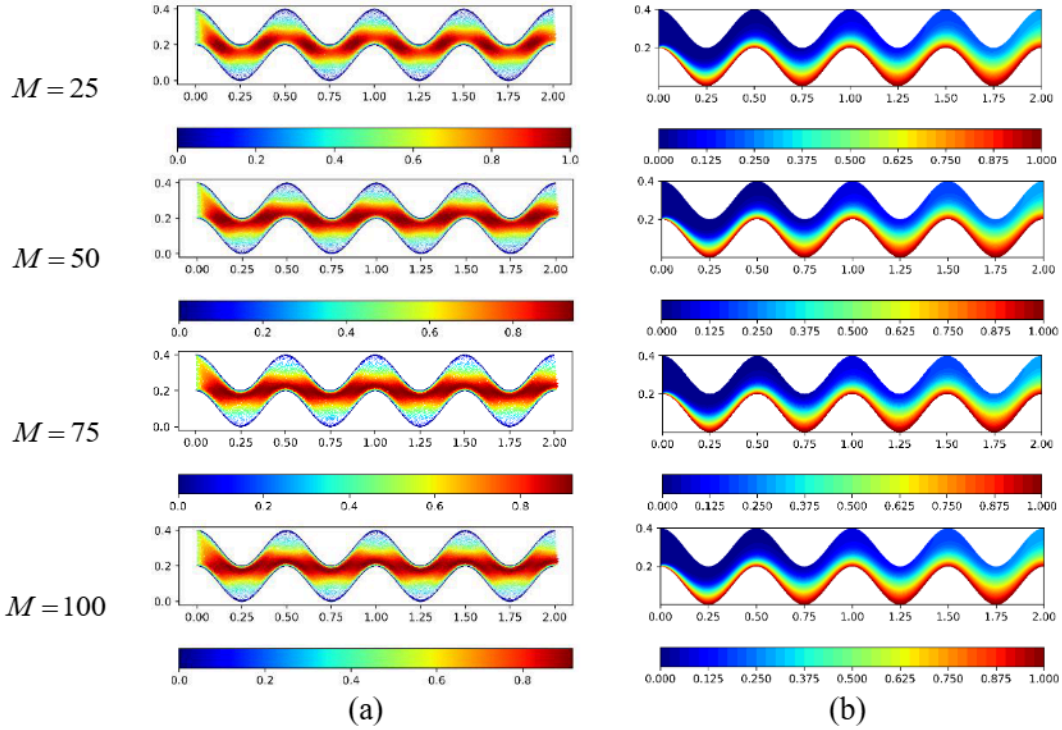

Figure 4: Variational of magnetic parameter, M, on (a) velocity and (b) temperature profiles

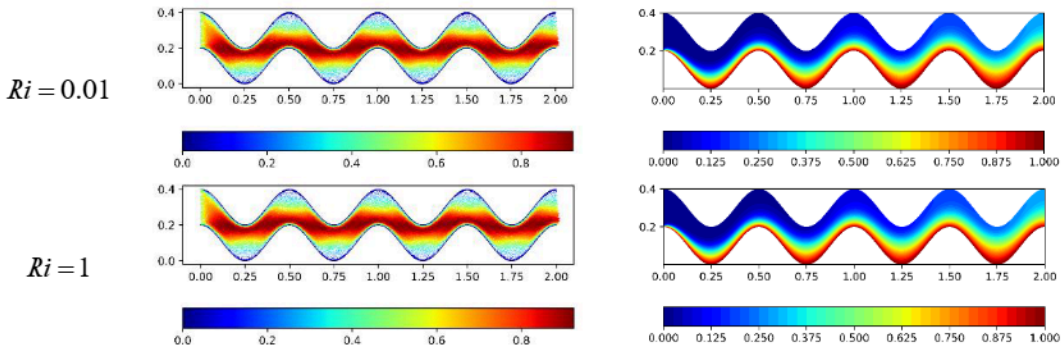

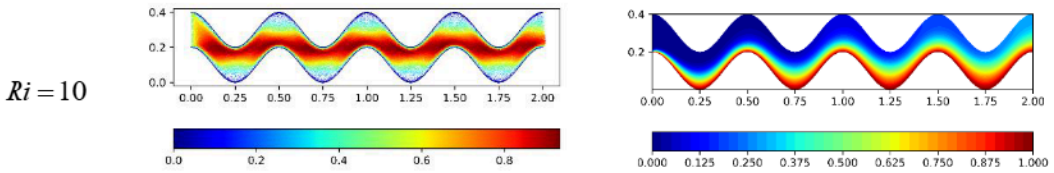

Figure 5: Variation of Richardson number, Ri, on (a) velocity and (b) temperature profiles

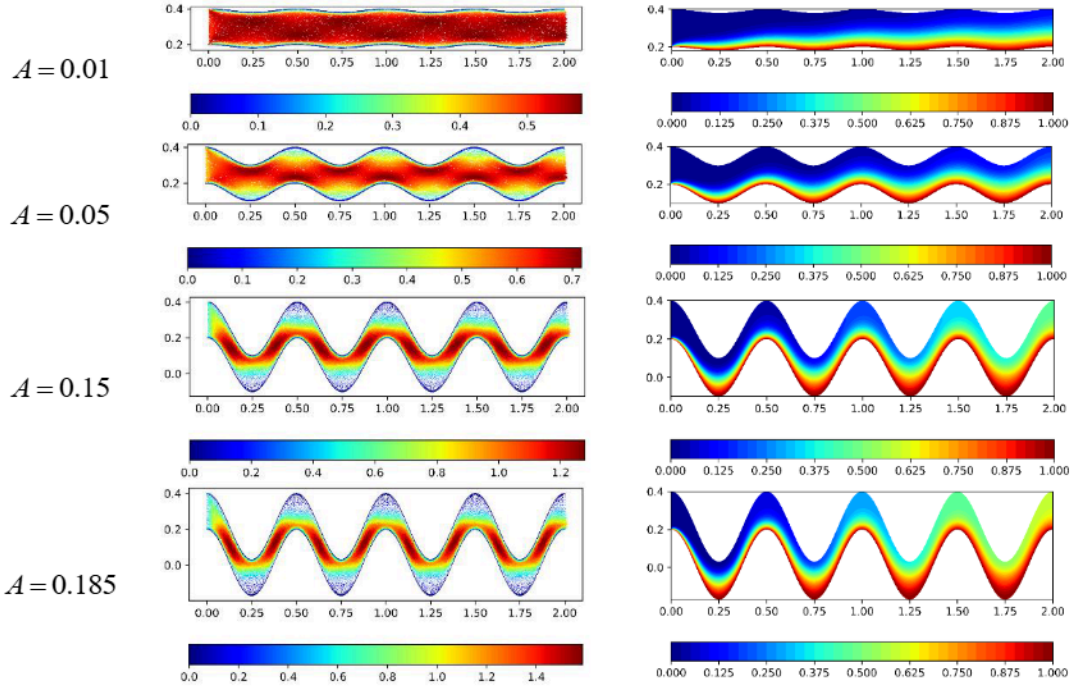

Figure 6: Variation of wavy wall amplitude, A, on (a) velocity and (b) temperature profiles

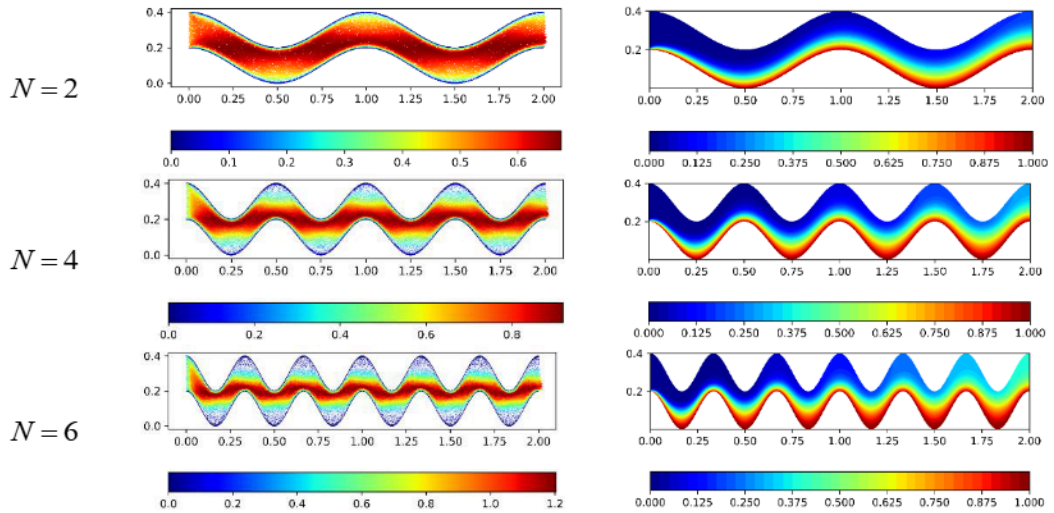

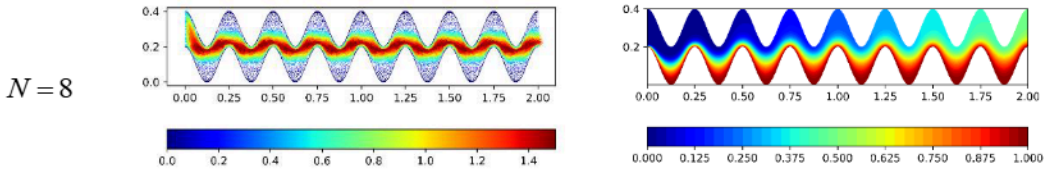

(a) (b)

Figure 7: Variation of undulation number of wavy surfaces, N, on (a) velocity and (b) temperature profiles

Conclusion

To summarize, this study investigates the effects of MHD, Richardson number, wavy wall amplitude, and undulation number of wavy surfaces on the velocity and the temperature profiles in a wavy channel. Using the standard Galerkin method to get the weak formulation of the continuity equation [Eq. (5)], the momentum equation [Eq. (6)], the energy equation [Eq. (7)]. Then, solve the equations with the help of the automated solutions technique FEniCS. The results show that the velocity profiles increase with the increment of Richardson number, wavy walls amplitude, and undulation number of wavy surfaces. On the contrary, a boost in magnetic parameters shows a decline in the velocity profiles. Amplifying the wavy wall amplitude and undulation number shows a significant impact to the temperature profile. However, rising the magnetic parameter and Richardson number shows no notable change in the temperature profiles.

Acknowledgments

The authors would like to acknowledge the Ministry of Higher Education Malaysia and Research Management Centre, International Islamic University Malaysia (IIUM) for financial support through project ID FRGS/1/2019/STG06/UIAM/02/3.

Article History

Received: 15-05-2025
Accepted: 04-12-2025

References

Ahmed, M. A., Yusoff, M. Z., Ng, K. C., & Shuaib, N. H. (2015). Numerical and experimental investigations on the heat transfer enhancement in corrugated channels using SiO2–water nanofluid. *Case Studies in Thermal Engineering*, *6*, 77-92.

Alsabery, A. I., Sheremet, M. A., Chamkha, A. J., & Hashim, I. (2022). Forced convection of turbulent flow into the wavy parallel channel. *Journal of Thermal Analysis and Calorimetry*, *147*(20), 11183-11194.

Asimoni, N. R. M., Mohammad, N. F., Kasim, A. R. M., & Shafie, S. (2018, June). MHD forced convective flow past a vertical plate: An automated solution approach. In *AIP Conference Proceedings* (Vol. 1974, No. 1). AIP Publishing.

Abu Talib, A. R., Hilo, A. K. (2021). Fluid flow and heat transfer over corrugated backward facing step channel. *Case Studies in Thermal Engineering*, *24*, 100862.

Hussain, S., Qureshi, M. A., & Ahmed, S. E. (2023). Impact of wavy porous layer on the hydrodynamic forces and heat transfer of hybrid

nanofluid flow in a channel with cavity under the effect of partial magnetic field. *Journal of Non-Equilibrium Thermodynamics*, *48*(3), 255-269.

Iwatsu, R., Hyun, J. M., & Kuwahara, K. (1993). Mixed convection in a driven cavity with a stable vertical temperature gradient. *International Journal of Heat and Mass Transfer*, *36*(6), 1601-1608.

Izumi, R., Yamashita, H., & Oyakawa, K. (1983). Fluid flow and heat transfer in corrugated wall channels: 4th report, analysis in the case where channels are bent many times. *Bulletin of JSME*, *26*(217), 1146-1153.

Jalili, B., Azar, A. A., Jalili, P., Liu, D., Abdelmohimen, M. A., & Ganji, D. D. (2024). Investigation of the unsteady MHD fluid flow and heat transfer through the porous medium asymmetric wavy channel. *Case Studies in Thermal Engineering*, *61*, 104859.

Lahlou, S., Boulahia, Z., & Sehaqui, R. (2024). Forced convection Heat transfer enhancement and entropy generation of non-Newtonian CNT–water nano-fluid in a channel with a wavy bottom wall. *International Journal of Thermofluids*, *24*, 100980.

Larson, M. G., & Bengzon, F. (2013). *The finite element method: theory, implementation, and applications* (Vol. 10). Springer Science & Business Media.

Logg, A., Mardal, K. A., & Wells, G. (Eds.). (2012). *Automated solution of differential equations by the finite element method: The FEniCS book* (Vol. 84). Springer Science & Business Media.

Madlool, N. A., Alshukri, M. J., Alsabery, A. I., Eidan, A. A., & Hashim, I. (2023). Numerical analysis of transfer of heat by forced convection in a wavy channel. *Int J Renew Energy Dev*, *12*, 155-65.

Mehta, S. K., Pati, S., & Baranyi, L. (2022). Effect of amplitude of walls on thermal and hydrodynamic characteristics of laminar flow through an asymmetric wavy channel. *Case Studies in Thermal Engineering*, *31*, 101796.

Pati, S., Mehta, S. K., & Borah, A. (2017). Numerical investigation of thermo-hydraulic transport characteristics in wavy channels: comparison between raccoon and serpentine channels. *International Communications in Heat and Mass Transfer*, *88*, 171-176.

Their, K. M., Azeez, K., & Mohsin, M. A. (2023). Thermohydraulic performance study of the effect of winglet inserts and a corrugated wall in a rectangular channel. *Case Studies in Thermal Engineering*, *52*, 103707.

Zhang, J., Kundu, J., & Manglik, R. M. (2004). Effect of fin waviness and spacing on the lateral vortex structure and laminar heat transfer in wavy-plate-fin cores. *International Journal of Heat and Mass Transfer*, *47*(8-9), 1719-1730.